Order and Composition of Methyl-Carboxyl and Methyl-Hydroxyl Surface-Chemical Gradients

Nagaiyanallur V. Venkataraman, Stefan Zürcher, and Nicholas D. Spencer*

Laboratory for Surface Science and Technology, Department of Materials, ETH Zurich, Wolfgang-Pauli-Strasse 10, CH-8093 Zurich, Switzerland

Received December 6, 2005. In Final Form: February 14, 2006

A detailed infrared and XPS characterization of surface-chemical gradients of dodecanethiol with 11-mercaptoundecanol or 11-mercaptoundecanoic acid self-assembled on gold, is reported. Gradients were prepared using a simple, two-step process previously reported from our laboratory, which involves a controlled immersion of a polycrystalline gold substrate in a dilute (5 μM) solution of one component and a subsequent back-filling with the other. FTIR measurements show that a single-component gradient of dodecanethiol is composed of disordered, liquidlike alkyl chain conformations. Such a gradient, when back-filled with a complementary thiol, having either a hydroxyl or carboxyl end-group, yields two-component gradients that show similar changes in wettability along their lengths. However, while gradients composed of methyl and hydroxyl end-groups show a well-ordered alkyl chain structure over their entire length, methyl-carboxyl gradients exhibit a greater conformational disordering toward the carboxyl-rich end.

Introduction

The self-assembly of long-chain amphiphilic molecules on solid surfaces has been extensively studied as a convenient route to surface modification;[1−5] of particular interest are self-assembled monolayers (SAMs) formed by long-chain alkanethiols on gold due to their high stability and ease of preparation.[6,7] Many applications of alkanethiol SAMs can be attributed to their utility in controlling macroscopic surface properties, such as wettability,[8,9] adhesion, or friction,[10,11] by a simple change of the chemical functional group at the alkyl chain termini. A systematic variation in surface properties can be achieved by coadsorption of two dissimilarly end-functionalized thiols from solution, and numerous investigations have been carried out on such two-component mixed SAMs of thiols on gold with a variety of combinations of end-groups including $-CH_3$, $-OH$, $-COOH$, $-NH_2$, $-CF_3$, $-CONH_2$, ferrocene, and oligo(ethylene glycol).[8,9,12−19] Surfaces with such well-defined surface-chemical compositions are useful for a systematic study of many interesting surface phenomena. Surfaces exhibiting changes in chemical composition within a single sample are of interest since they allow for an array of surface compositions to be explored within a single experiment. There have been several methods described previously for the preparation of such gradient surfaces with varying surface-chemical composition over a length of a few centimeters.[20] The earliest of such gradients reported include the wettability gradients based on silane adsorption on silica.[21−23] Surface-chemical gradients from SAMs of thiols on gold have also been prepared using several different methods such as cross-diffusion of two differently end-functionalized thiols in a polysaccharide matrix,[24,25] electrochemical desorption of thiol monolayers,[26] mass-transfer limited microcontact printing,[27] and UV/ozone treatment of SAMs.[28] The use of gradient surfaces to explore several surface compositions in a single measurement had been demonstrated in studies of surfactant and protein adsorption on a wettability gradient,[21,29] optimizing the immobilization of streptavidin and in relation to protein repellency of oligo(ethylene glycol)-terminated surfaces.[30] Surface-chemical gradients have also been used to prepare a gradient in surface

* To whom correspondence should be addressed. E-mail: nicholas.spencer@mat.ethz.ch. Fax: +41 44 633 10 27.

(1) Allara, D, L.; Nuzzo, R. G. *Langmuir* **1985**, *1*, 45.
(2) Allara, D. L.; Nuzzo, R. G. *Langmuir* **1985**, *1*, 52.
(3) Porter, M. D.; Bright, T. B.; Allara, D. L.; Chidsey, C. D. E. *J. Am. Chem. Soc.* **1987**, *109*, 3559.
(4) Bain, C. D.; Whitesides, G. M. *Angew. Chem., Int. Ed. Engl.* **1989**, *28*, 506.
(5) Bain, C. D.; Troughton, B. E.; Tao, Y.-T.; Evall, J.; Whitesides, G. M.; Nuzzo, R. G. *J. Am. Chem. Soc.* **1989**, *111*, 321.
(6) Ulman, A. *Chem. Rev.* **1996**, *96*, 1533.
(7) Love, J. C.; Estroff, L. A.; Kriebel, J. K.; Nuzzo, R. G.; Whitesides, G. M. *Chem. Rev.* **2005**, *105*, 1103.
(8) Nuzzo, R. G.; Dubois, L. H.; Allara, D. L. *J. Am. Chem. Soc.* **1990**, *112*, 558.
(9) Dubois, L. H.; Zergaski, B. R.; Nuzzo, R. G. *J. Am. Chem. Soc.* **1990**, *112*, 570.
(10) Kim, H. I.; Graupe, M.; Oloba, O.; Koini, T.; Imaduddin, S.; Lee, T. R.; Perry, S. S. *Langmuir* **1999**, *15*, 3179.
(11) Perry, S. S.; Lee, S.; Shon, Y.-S.; Colorado, R., Jr.; Lee, T. R. *Tribol. Lett.* **2001**, *10*, 81.
(12) Bain, C. D.; Whitesides, G. M. *J. Am. Chem. Soc.* **1988**, *110*, 6560.
(13) Bain, C. D.; Evall, J.; Whitesides, G. M. *J. Am. Chem. Soc.* **1989**, *111*, 7155.
(14) Ulman, A.; Evans, S. D.; Shnidman, Y.; Sharma, R.; Eilers, J. E. *Adv. Coll. Int. Sci.* **1992**, *39*, 175.
(15) Laibinis, P. E.; Whitesides, G. M. *J. Am. Chem. Soc.* **1992**, *114*, 1990.
(16) Balamurugan, S.; Ista, L. K.; Yan, J.; Lopez, G. P.; Fick, J.; Himmelhaus, M.; Grunze, M. *J. Am. Chem. Soc.* **2005**, *127*, 14548.
(17) Auletta, T.; van Veggel, F. C. J. M.; Reinhoudt, D. N. *Langmuir* **2002**, *18*, 1288.
(18) Li, S.; Cao, P.; Colorado, R. Jr.; Yan, X.; Wenzl, I.; Shmakova, O. E.; Graupe, M.; Lee, T. R.; Perry, S. S. *Langmuir* **2005**, *21*, 933.
(19) Tsao, W.-M.; Hoffmann, C. L.; Rabolt, J. F.; Johnson, H. E.; Castner, D. G.; Erdelen, C.; Ringsdorf, H. *Langmuir* **1997**, *13*, 4317.
(20) Busscher, H. J.; Elwing, H. *Colloids Surf., B* **1999**, *15*, 1 and references therein.
(21) Elwing, H.; Welin, S.; Askendal A.; Nilsson, U.; Lundstrom, I. *J. Colloid Interface Sci.* **1987**, *119*, 203.
(22) Welin-Klintstrom, S.; Askendal, A.; Elwing, H. *J. Colloid Interface Sci.* **1993**, *158*, 188.
(23) Golander, G. C.; Caldwell, K.; Lin, Y. S. *Colloids Surf.* **1989**, *42*, 165.
(24) Liedberg, B.; Tengvall, P. *Langmuir* **1995**, *11*, 3821.
(25) Lestelius, M.; Engquist, I.; Tengvall, P.; Chaudhury, M. K.; Liedberg, B. *Colloids Surf., B* **1999**, *15*, 57.
(26) Plummer, S. T.; Wang, Q.; Bohn, P. W.; Stockton, R.; Schwartz, M. A. *Langmuir* **2003**, *19*, 7528.
(27) Kraus, T.; Stutz, R.; Balmer, T, E.; Schmid, H.; Malaquin, L.; Spencer, N. D.; Wolf, H. *Langmuir* **2005**, *21*, 7796.
(28) Loos, K.; Kennedy, S. B.; Eidelman, N.; Tai, Y.; Zharnikov, M.; Amis, E. J.; Ulman, A.; Gross, R. A. *Langmuir* **2005**, *21*, 5237.
(29) Welin-Klintstrom, S.; Lestelius, M.; Liedberg, B.; Tengvall, P. *Colloids Surf., B* **1999**, *15*, 81.
(30) Riepl, M.; Ostblom, M.; Lundstrom, I.; Svensson, S. C. T.; Denier van der Gon, A. W.; Schaferling, M.; Liedberg, B. *Langmuir* **2005**, *21*, 1042.

10.1021/la053302t CCC: $33.50
Published on Web 03/23/2006

density of nanoparticles[31] and proteins[26] by utilizing the differences in chemical reactivity of the terminal functional group.

An alternative method of preparation of a two-component surface-chemical gradient of alkanethiols on gold was recently reported from our laboratory.[32] The method utilizes the kinetics of adsorption of dodecanethiol from very dilute solution (5 μM) by a controlled immersion step producing a gradient in concentration of dodecanethiol molecules on the surface, followed by back-filling with 11-mercaptoundecanol. The surface composition of hydroxyl- and methyl-terminated thiols has been shown to vary almost linearly along the length of a 4-cm-long polycrystalline gold surface. This method is simple and could, in principle, be extended to any combination of end-functional groups and sample size by appropriately controlling the thiol concentrations and immersion speeds. Here we demonstrate the ease of this method to produce chemical functionality gradients with different end-groups and report a detailed structural characterization of these gradients using contact angle measurements, X-ray photoelectron spectroscopy, and infrared spectroscopy. We report gradients composed of methyl-hydroxyl and methyl-carboxyl end-groups, which both show similar, linear changes in wettability with water. The deprotonation of the carboxyl groups allows one to produce surfaces with well-controlled gradients in surface charge, which could also be of interest in many surface-interaction studies, such as the field of protein adsorption.[30] Moreover, since carboxyl-terminated SAMs have been shown to be useful for surface immobilization of several interesting species ranging from simple bivalent metal ions[33] to magnetic nanoclusters,[34,35] polymers,[36] and proteins,[26] carboxyl-terminated gradients open the door to innumerable, more complex, and technologically relevant gradient systems.

Experimental Section

Dodecanethiol, 11-mercaptoundecanoic acid, and 11-mercaptoundecanol were obtained from Aldrich and used as received. Ethanol (Fluka) was used as solvent for all preparations. The substrates, 2 $\times$ 4 cm silicon wafers (POWATEC, Cham, Switzerland) were cleaned with oxidizing piranha solution, a 7:3 mixture of concentrated H_2SO_4 and 30% H_2O_2 (C*aution: piranha solution reacts violently when contacted with organic molecules and should be handled with extreme care*), thoroughly rinsed with copious amounts of MilliQ water (>18 MΩ), subsequently cleaned with O_2 plasma (2 min O_2, high power, Harrick Plasma Cleaner/Sterilizer), and covered with a 6-nm adhesive layer of chromium before evaporation of 80-nm-thick layer of gold (MED020 coating system, BALTEC, Balzers, Lichtenstein). Prior to the immersion step, the substrates were cleaned for 30 s in N_2 plasma (30 s, high power) and left in pure ethanol for 10 min. Gradients were formed by controlled immersion of the substrate into a dilute (5 μM) ethanolic solution of dodecanethiol, the speed of immersion (75 μm/s) being accurately controlled by a linear-motion drive (OWIS, Staufen, Germany). The sample was quickly removed from the thiol solution and thoroughly rinsed with ethanol to remove physisorbed and loosely bound thiol molecules. The sample was then immersed in an ethanolic solution (0.01 mM) of 11-mercaptoundecanol or 11-mercaptoundecanoic acid overnight followed by thorough rinsing with ethanol and drying in a flow of high-purity N_2. Gradients made from 11-mercaptoundecanoic acid were, additionally, rinsed with acidified ethanol and dried in a flow of N_2.

Contact Angle Measurements. Dynamic contact angles were measured employing a contact angle goniometer (G2/G40 2.05-D, Kruss GmBH, Hamburg, Germany). Advancing and receding contact angles were determined using digital image analysis. Measurements were carried out every 5 mm along the substrate. All contact-angle measurements were averaged over several samples.

XPS Measurements. XPS analyses were performed using a VG Theta Probe spectrophotometer (Thermo Electron Corporation, West Sussex, UK) equipped with a concentric hemispherical analyzer and a two-dimensional channel plate detector with 112 energy and 96 angle channels. Spectra were acquired at a base pressure of 10^{-9} mbar or below using a monochromatic Al Kα source with a spot size of 300 μm. The instrument was run in the standard lens mode with electrons emitted at 53° to the surface normal and an acceptance angle of $\pm$30°. The analyzer was used in the constant analyzer energy mode. Pass energies used for survey scans and detailed scans were 200 and 100 eV, respectively, for gold Au4f, carbon C1s, oxygen O1s, and sulfur S2p. Under these conditions, the energy resolution (full width at half-maximum height, fwhm) measured on gold $Au4f_{7/2}$ is 1.95 and 0.82 eV, respectively. Acquisition times were approximately 5 min for survey scans and 30 min (total) for high-energy-resolution elemental scans. These experimental conditions were chosen in order to obtain an adequate signal-to-noise ratio in a minimum time and to limit beam-induced damage. Under these conditions, sample damage was negligible, and reproducible analyzing conditions were obtained on all samples. All recorded spectra were referenced to the gold $Au4f_{7/2}$ signal at 83.96 eV. Data were analyzed using the program CasaXPS [Version 2.3.5, www.casaxps.com]. The signals were fitted using Gaussian−Lorentzian functions and Tauc asymmetry in the case of gold and least-squares-fit routines following Shirley iterative background subtraction. Sensitivity factors were calculated using published ionization cross sections[37] corrected for the angular asymmetry[38] and the attenuation length dependence with kinetic energy.

Infrared Spectroscopy. Polarization-modulation infrared reflection−absorption spectra (PM-IRRAS) were recorded on a Bruker IFS 66v IR spectrometer, equipped with a PMA37 polarization-modulation accessory (Bruker Optics, Germany). The interferogram from the spectrometer's external beam port was passed through a KRS-5 wire-grid polarizer and a ZnSe photoelastic modulator before reflecting off the sample surface at an angle of 80° and being detected with a liquid-nitrogen-cooled MCT detector. The frequency of polarization modulation was 50 kHz, with a maximum of polarization retardation set at 3000 cm^{-1}. The sample compartment was continuously purged with dry air. The sample holder was suitably modified to be able to record spectra of different regions of the gradient with a 2-mm aperture. Typically, 1024 scans of multiplexed interferograms were collected with 4-cm^{-1} resolution and processed with the OPUS software (Bruker Optics, Germany). The spectra were background-corrected with a polynomial.

Results and Discussion

The advancing and receding water-contact angles measured along a gradient of 1-dodecanethiol that had been back-filled with 11-mercaptoundecanoic acid (methyl-carboxyl gradient) are plotted in Figure 1. The adsorption parameters had been chosen, as described in our earlier publication,[32] such that the coverage varies almost linearly along the gradient axis, resulting in linear variation of the water-contact angles upon back-filling with the complementary thiol. The advancing contact angle at the methyl-rich end is about 80°, decreasing almost linearly along the length of the gradient, and reaches a value of about 40° at the carboxyl-rich end. The hysteresis in contact angle was between 10° and 15° along the length of the gradient, similar to those observed on a gradient prepared from dodecanethiol and 11-mercaptoundecanol[32] (methyl-hydroxyl gradient). For compari-

(31) Bhat, R. R.; Genzer, J.; Chaney, B. N.; Sugg, H. W.; Liebmann-Vinson, A. *Nanotechnology* **2003**, *14*, 1145.
(32) Morgenthaler, S.; Lee, S.; Zürcher, S.; Spencer, N. D. *Langmuir* **2003**, *19*, 10459.
(33) Yang, K.-L.; Cadwell, K.; Abbott, N. L. *Adv. Mater.* **2003**, *15*, 1819.
(34) Naitabdi, A.; Bucher, J.-P.; Gerbier, P.; Rabu, P.; Drillon, M. *Adv. Mater.* **2005**, *17*, 1612.
(35) Steckel, J. S.; Persky, N. S.; Martinez, C. R.; Barnes, C. L.; Fry, E. A.; Kulkarni, J.; Burgess, J. D.;. Pacheco, R. B.; Stoll, S. L. *Nano Lett.* **2004**, *4*, 399.
(36) Barreira, S. V. P.; Silva, F. *Langmuir* **2003**, *19*, 10324.
(37) Scofield, J. H. *J. Electron Spectrosc. Relat. Phenom.* **1976**, *8*, 129.
(38) Reilman, R. F.; Msezane, A.; Manson, S. T. *J. Electron Spectrosc. Relat. Phenom.* **1976**, *8*, 389.

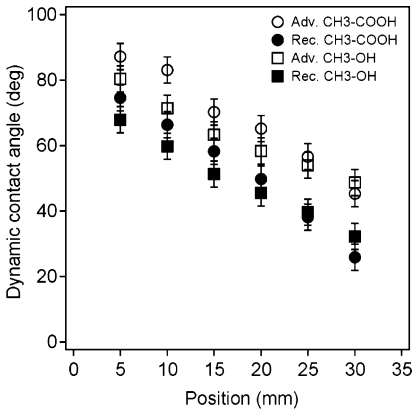

Figure 1. Advancing (open symbols) and receding (filled symbols) water contact angles on a methyl-carboxyl (circles) and a methyl-hydroxyl (squares) gradient measured along the length.

son, the contact angles measured on a methyl-hydroxyl gradient are also shown in Figure 1. It may be noted that the contact angles seen at the two extremities of the gradient are quite different from those observed on full monolayers of either of the two components (>110° for dodecanethiol and <10° for 11-mercaptoundecanoic acid), indicating that the gradients do not span the entire composition range. This is attributed to the fact that the single-component gradient formed after the first immersion step (as will be shown below from XPS measurements) never attains full coverage even at the highest-concentration end due to the low concentration of thiol used and the relatively short immersion times. Also, some replacement of the adsorbed dodecanethiol molecules by the 11-mercaptoundecanoic acid is expected during the second immersion step. However, substantial replacement of adsorbed thiol molecules by a second thiol is unlikely due to the low concentrations of the thiols employed during back-filling step.

XPS. X-ray photoelectron spectra in the C1s and O1s regions measured at 5 mm intervals on a methyl-carboxyl gradient are shown in Figure 2. The spectra in the C1s region show an intense peak at 285.0 eV (not shown in the spectra), corresponding to the C1s of the aliphatic chain with a less-intense component at 286.7 eV assigned to the C1s of the CH_2 group closest to either the S or COOH group. The peak at 289.7 eV is assigned to the C1s of the carboxyl group. The intensity of this peak increases along the gradient from the methyl-rich end to the carboxyl-rich end. The spectra shown here are for the samples prepared by rinsing with acidified ethanol after the second immersion step. This ensures the complete protonation of the carboxyl group, as shown by the O1s spectra in Figure 2b. Two oxygen species can be detected with an area ratio of nearly 1:1. These two peaks can be assigned to the C**═O** and the C−**O**H oxygens of the carboxyl group. When the gradients were rinsed with acid-free ethanol, an additional component for the carbon peak could be detected at 288.8 eV. This peak is assigned to a deprotonated carboxylate species, the intensity of which indicates that ∼50% of all carboxyl groups had been deprotonated. Previous studies on full monolayers of carboxyl-terminated thiols on gold prepared from ethanol have shown that carboxyl groups are generally deprotonated and exist as carboxylates, often with the presence of trace amounts of metal ions, typically sodium, as counterion.[39,40] Often, in our measurements when no acid rinsing step was employed, contamination with low concentrations of bivalent metal ions, such as zinc, could be detected and a third oxygen species and a new carbon species that are attributed to carboxylate were observed.

In general, there is somewhat more oxygen and less sulfur detected than expected for the stoichiometric amount calculated for the adsorbed molecules. This is a consequence of the orientation of the carboxylic acids toward the vacuum−SAM interface, leading to the sulfur being buried underneath the SAM. Also, angle-resolved measurements show that this deviation is more pronounced for grazing-angle electron detection than for angles closer to the surface normal, as would be expected. The presence of other oxygen species, such as adsorbed water, H_3O^+, or oxidized gold cannot be completely excluded. The positions and widths of all the species are summarized in Table 1.

Quantification of the intensities of the various species was performed according to the procedure described above. These are shown in Figure 3a, for different positions along the gradient. The carbon intensity decreases, while that of oxygen increases linearly along the length of the gradient. A quantitative differentiation between the aliphatic thiol and the carboxy thiol is very difficult due to the weakness of the carboxylate signal in comparison to the aliphatic carbon and the uncertainty of the presence of other oxygen species on the samples. Also shown in Figure 3b are the intensity ratios of the overlayer over the substrate intensity calculated as $\sum(I_{S2p} + I_{C1s} + I_{O1s})/I_{Au4f}$. This ratio is directly related to the thickness of the overlayer[41] and therefore a measure for the coverage. As can be seen in Figure 3b, for a back-filled monolayer, this intensity ratio stays nearly constant over the entire length of the gradient and is comparable to the values obtained for single-component SAMs of either dodecanethiol or 11-mercaptoundecanoic acid (shown at the two extremes of the plot). Whereas in the case of a non-back-filled gradient, the ratio is decreasing, starting at ∼80% going down to ∼30% of the value of a full monolayer. Due to rapid contamination of the uncovered regions with adventitious carbon, the real thiol coverage on the low-coverage side could be even lower than the measured value. This could also be seen from the increase of the carbon-to-sulfur ratio with decreasing coverage (data not shown). Similar arguments of contamination with adventitious carbon could also explain the slightly larger values seen on the carboxyl side of the back-filled gradient (position 30 mm). Another feature of the plot shown in Figure 3b is the measure of compositional homogeneity of the gradients. For three of the positions along the single-component gradient (positions at 7.5, 19.5, and 32 mm), intensity ratios are also shown from measurements at five different locations along the direction perpendicular to the gradient direction. The variations in the intensity ratios are within the experimental uncertainties, indicating that the gradients are homogeneous along the perpendicular axis.

Infrared Spectroscopy. Infrared spectroscopy has been shown to be a useful method to study structure of self-assembled thiol monolayers, especially the orientation[42] and conformation[3] of the alkyl chains. PM-IRRA spectra of a single-component dodecanethiol gradient measured at every 5 mm along the length of the gradient are shown in Figure 4. The most prominent features in the spectra could be readily assigned to the C−H stretching modes arising from the $-CH_2-$ groups and the terminal CH_3 groups[2,3,5]. Peaks at ∼ 2850 and ∼ 2920 cm^{-1} are assigned to the CH_2 symmetric and antisymmetric stretching modes and the peaks at 2880 and 2960 cm^{-1} to the symmetric and asymmetric stretching modes of the CH_3 group, respectively. At the lowest-

(39) Arnold, R.; Azzam, W.; Terfort, A.; Woll, C. *Langmuir* **2002**, *18*, 3980.
(40) Willey, T. M.; Vance, A. L.; van Buuren, T.; Bostedt, C.; Nelson, A. J.; Terminello, L. J.; Fadley, C. S. *Langmuir* **2004**, *20*, 2746.
(41) Fadley, C. S. *Prog. Surf. Sci.* **1984**, *16*, 275.
(42) Parikh, A. N.; Allara, D. L. *J. Chem. Phys.* **1992**, *96*, 927.

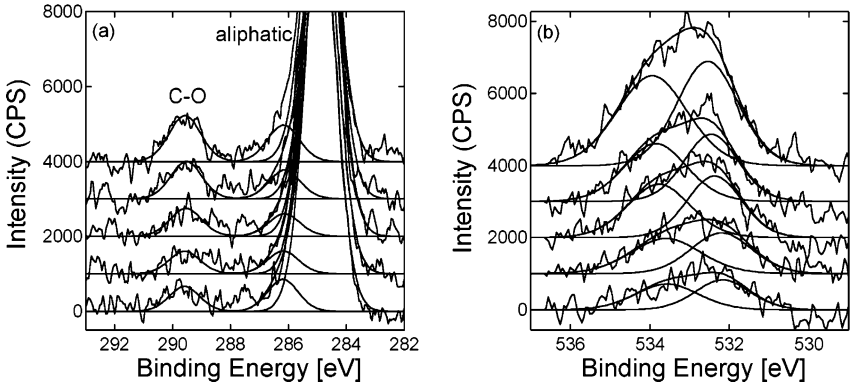

Figure 2. X-ray photoelectron spectra in the (a) C1s and (b) O1s regions measured on a methyl-carboxyl gradient. Spectra shown are measured from the methyl-rich end (bottom) to the carboxyl rich end (top) at 4, 11, 18, 25, and 34 mm from the methyl-rich end. The C1s region is expanded to highlight the change in the C−O intensity. The spectra are displaced along the *y* axis by 1000 CPS for clarity.

Table 1. Positions and Widths of Important XPS Peaks

	average binding energy (eV)	fwhm
$Au4f_{7/2}$	83.96	0.82
$Au4f_{5/2}$	87.69	0.91
C1s aliphatic	285.02	1.45
C1s CH_2-S/CH_2-COOH	286.72	1.45
C1s COOH	289.72	1.45
O1s C═O	532.41	1.61
O1s C−OH	533.81	1.86
$S2p_{3/2}$	162.12	1.00
$S2p_{1/2}$	163.30	1.00

concentration end (top trace) of the gradient, a shoulder around 2900 cm^{-1} could be seen, which could be due to a Fermi resonance involving the bending modes and the symmetric stretch or to a methylene antisymmetric stretch arising from the CH_2 groups nearest to the sulfur atoms.[43]

The symmetric and the antisymmetric stretching modes of the CH_2 groups appear at 2854 and 2924 cm^{-1} through the entire sample length. It is well known in the literature from a variety of studies on the structure of alkyl-chain assemblies, such as crystalline *n*-alkanes,[44,45] lipids, and SAMs,[46] that these vibrational modes are sensitive to conformational order of the alkyl chain. In a crystalline, all-trans conformation, the modes appear in the regions 2914−2918 and 2846−2848 cm^{-1} for the methylene antisymmetric and symmetric stretching modes,[45] respectively, shifting progressively to higher wavenumbers with increasing disorder and appearing in the region 2924−2926 cm^{-1} for the antisymmetric and 2854−2858 cm^{-1} for the symmetric stretching modes.[44] This indicates that, on the single-component dodecanethiol gradient, the alkyl chain possesses a disordered liquidlike conformation over the entire length of the gradient. This is expected, since at such low concentration (5 μM) and relatively short immersion times, of the order of a few minutes, the monolayer is expected to be composed of a mixture of lying-down and standing-up molecules with a considerable amount of disorder. Nevertheless, it should be noted that, even at the most concentrated end, the spectrum does not resemble that of a complete monolayer (shown as a dotted line in Figure 4) in terms of the intensity ratios of the methyl symmetric to methylene symmetric stretching modes, as well as in the position of the methylene stretching modes. This indicates that the structure of the monolayer, even at the highest-concentration end, is far from crystalline and ordered. The intensity of the CH_3 symmetric stretching mode at 2880 cm^{-1} further illustrates this fact. This vibrational mode has a transition moment along the C−C bond axis of the terminal $-CH_2-CH_3$ bond, and its intensity relative to the overall intensity of the C−H stretching modes increases rapidly toward the higher-concentration end of the gradient. Apart from changes in this intensity due to increasing concentration of thiols on the surface (as shown by the XPS intensity ratios in Figure 3b), this nonlinear increase toward the high-concentration end of the gradient could be due to a change in orientation of the adsorbed thiol molecules from a lying-down phase at the less-concentrated end to a standing-up phase. AFM measurements on such a gradient showed an islandlike structure with a typical height difference of 1 nm, consistent with the fact that the islands are surrounded by a disordered lying-down phase rather than bare gold.[47] This is not surprising considering the fact that the structure of thiol monolayers is known to evolve over long time scales and infrared spectral intensity changes in uniform SAMs have been reported over several hours/days.[48] The changes in intensity observed here are similar to ex situ infrared measurements on incomplete thiol monolayers prepared from dilute concentrations.[49] A detailed description of the structure of such a gradient at sub-micrometer length scales obtained with atomic force microscopy has been recently reported elsewhere.[47]

Infrared spectra of a two-component, methyl-hydroxyl gradient, prepared by back-filling a single-component dodecanethiol gradient with 11-mercaptoundecanol, are shown in Figure 5a. The most noticeable feature in the series of spectra, measured at different positions along the length of the gradient, is the change in the intensity of C−H stretching modes of the terminal CH_3 groups at 2960 cm^{-1}. The intensity of this band, as expected, decreases along the length of the gradient moving from the methyl-rich end to the hydroxyl-rich end. This correlates well with the changes observed in the contact angles and XPS measurements. The apparent increase in the intensity at 2880 cm^{-1} band toward the hydroxyl side of the gradient could be due to the presence of an additional band, often observed in full monolayers of 11-mercaptoundecanol, assigned to the stretching mode of $-CH_2$ group adjacent to −OH.[8,50] The most important difference in the series of spectra on a methyl-hydroxyl gradient shown above, in comparison to the single-component gradient, is the position

(43) Parikh, A. N.; Gilmor, S. D.; Beers, J. D.; Beardmore, K. M.; Cutts, R. W.; Swanson, B. I. *J. Phys. Chem. B* **1999**, *103*, 2850.
(44) Snyder, R. G.; Strauss, H. L.; Elliger, C. A. *J. Phys. Chem.* **1982**, *86*, 5145.
(45) MacPhail, R. A.; Strauss, H. L.; Snyder, R. G.; Elliger, C. A. *J. Phys. Chem.* **1984**, *88*, 334.
(46) Nuzzo, R. G.; Korenic, E. M.; Dubois, L. H. *J. Chem. Phys.* **1990**, *93*, 767.
(47) Morgenthaler, S. M.; Lee, S.; Spencer, N. D. *Langmuir* **2006**, *22*, 2706.
(48) Terrill, R. H.; Tanzer, T. A.; Bohn, P. W. *Langmuir* **1998**, *14*, 845.
(49) Bensebaa, F.; Voicu, R.; Huron, L.; Ellis, T. H.; Kruus, E. *Langmuir* **1997**, *13*, 5335.
(50) Atre, S. V.; Leidberg, B.; Allara, D. L. *Langmuir* **1995**, *11*, 3882.

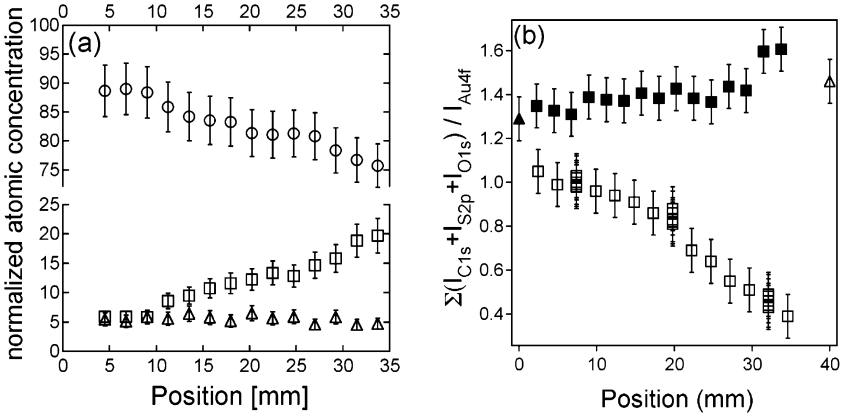

Figure 3. (a) Normalized atomic concentrations of the elements related to the SAM [carbon (circles), oxygen (squares) and sulfur (triangles)] along the length of a methyl-carboxyl gradient. The positions shown are the distances from the highest dodecanethiol concentration end. Error bars are estimated from the signal-to-noise ratios. (b) Film coverage determined by the ratio of the sum of S2p, C1s, and O1s intensities to substrate (Au4f) intensity along the length of a methyl-carboxyl (filled squares), single component (open squares) gradients compared to full monolayers of dodecanthiol (filled triangle) and 11-mercaptoundecanoic acid (open triangle). The intensity ratios at positions 7.5, 19.5, and 32 mm are also shown from measurements at five different locations along the perpendicular axis of the gradients to indicate the homogeneity of the gradients.

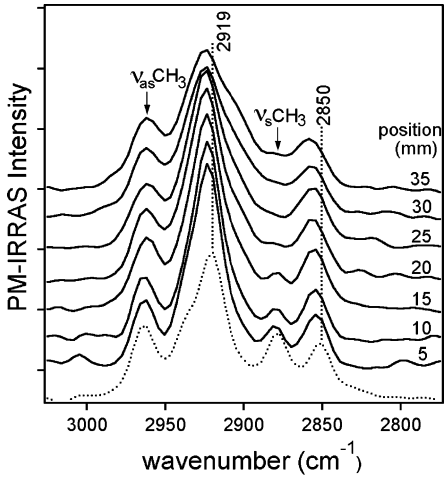

Figure 4. PM-IRRA spectra measured on a single-component 1-dodecanethiol gradient (solid lines) measured every 5 mm along the gradient from the high-concentration end (lower trace) to the low-concentration end (top). The spectra are displaced for clarity. The spectrum of a full monolayer of dodecanethiol (dotted line) is shown for comparison.

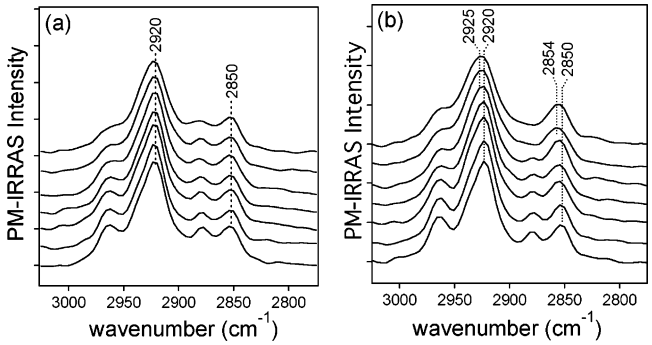

Figure 5. Infrared spectra of two-component gradients prepared from dodecanethiol back-filled with (a) 11-mercaptoundecanol and (b) 11-mercaptoundecanoic acid. The spectra shown are measured at 5 mm intervals along a 35-mm-long sample.

of the methylene stretching modes. Upon back-filling with 11-mercaptoundecanol, the symmetric and antisymmetric CH_2 stretching modes shift to 2850 and 2920 cm^{-1}, respectively. This indicates the establishment of a well-ordered monolayer throughout the entire length of the two-component gradient. Also, a slight decrease in the intensity of the methyl asymmetric stretching mode may be seen in the two-component gradients as compared to the single-component gradient. This is due to the replacement of dodecanethiol molecules by 11-mercaptoundecanol during the second immersion step. No quantitative analysis of the replacement kinetics from these intensities has been attempted here.

Infrared spectra in the C−H stretching region of a gradient back-filled with 11-mercaptoundecanoic acid are shown in Figure 5b. The intensities of the symmetric and asymmetric stretching modes of the methyl group decrease, as expected, from the CH_3-rich end to the COOH-rich end, in a similar way to that observed for a methyl-hydroxyl gradient. The positions of the methylene stretching modes also shift to lower wavenumbers compared to single-component gradients. This indicates a change in conformational ordering of the alkyl chains upon back-filling. However, in comparison to the methyl-hydroxyl gradient, the methylene stretching modes in the methyl-carboxyl gradient appear at higher wavenumbers at the carboxyl-rich end of the gradient. These modes appear at 2851 and 2921 cm^{-1} on the $-CH_3$ side of the sample, whereas they appear at 2854 and 2924 cm^{-1} at the −COOH end of the sample. The positions of the methylene stretching modes in all three gradients are plotted in Figure 6. This indicates that, while the methyl-hydroxyl gradient is conformationally well-ordered throughout its entire length, the methyl-carboxyl gradient shows an increasing conformational disorder toward the −COOH-rich end. The nature of the end functionality of thiol SAMs can significantly influence their packing, thereby modulating the conformational order of the alkyl chains.[51,52]

Carbonyl Stretching Region. Spectra in the 1900−1300 cm^{-1} region measured at different positions along a methyl-carboxyl gradient are shown in Figure 7. The spectra shown are those measured on an acid-rinsed sample. The spectra recorded on a sample prior to the acid-rinsing step are shown, for the same spectral region, as an inset. Two intense, broad bands centered around 1700 and 1450 cm^{-1} can be assigned to the carbonyl C═O stretching mode of a carboxylic acid and the symmetric stretching of carboxylate ion, respectively. The COO^- asymmetric

(51) Frey, S.; Shaporwnko, A.; Zharnikov, M.; Harder, P.; Allara, D. L. *J. Phys. Chem. B* **2003**, *107*, 7716.
(52) Dannenberger, O.; Weiss, K.; Himmel, H.-J.; Jager, B.; Buck, M.; Woll, C. *Thin Solid Films* **1997**, *307*, 183.

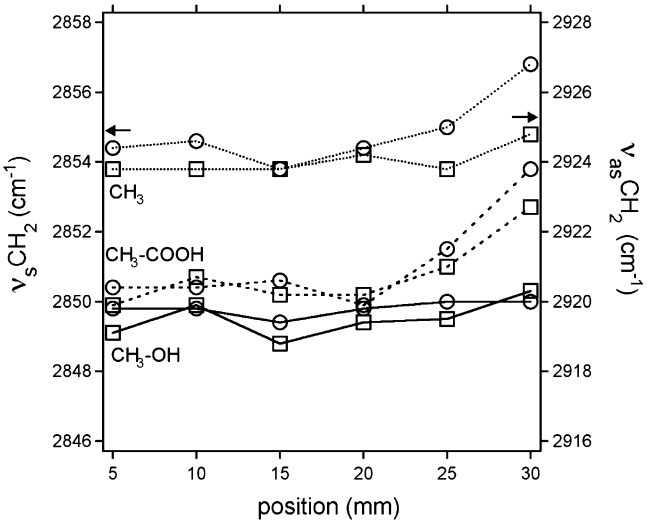

Figure 6. Positions of the methylene symmetric (circles) and antisymmetric (squares) stretching modes in single-component dodecanethiol gradients (dotted lines), and back-filled two-component gradients with 11-mercaptoundecanol (solid lines) and 11-mercaptoundecanoic acid (dashed line), along the length of the gradients.

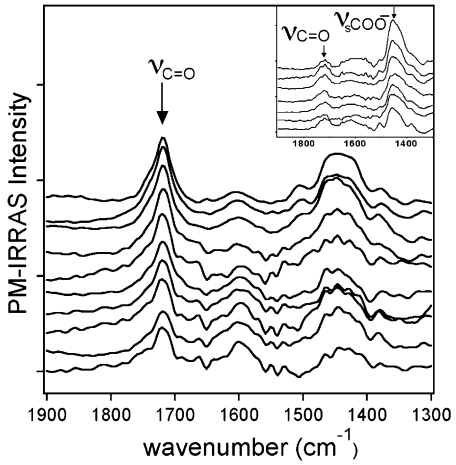

Figure 7. Infrared spectra of a methyl-carboxyl gradient in the carbonyl stretching region, showing the C═O stretching mode increasing in intensity along the length of the gradient moving to the carboxyl end. The inset shows spectra from the same region of a gradient prepared without the additional rinsing step with acidified ethanol, showing that the carboxyl groups are present predominantly as carboxylate species.

stretching band that appears in the region of 1570 cm^{-1} could not be clearly distinguished (inset spectra). From the inset spectra, it may thus be seen that the samples prepared from ethanol are almost exclusively composed of carboxylate species. This is in accordance with previous studies on −COOH-terminated monolayers and has been attributed to the presence of trace amounts of water and metal ions in the solvent.[39,40] A rinsing step with an ethanolic solution of HCl results in a predominantly carboxylic acid-terminated surface.[53] However, the intensity in the 1450−1600 cm^{-1} region does not go to zero upon rinsing with HCl.

(53) Methivier, C.; Beccard, B.; Pradier, C. M. *Langmuir* **2003**, *19*, 8807.

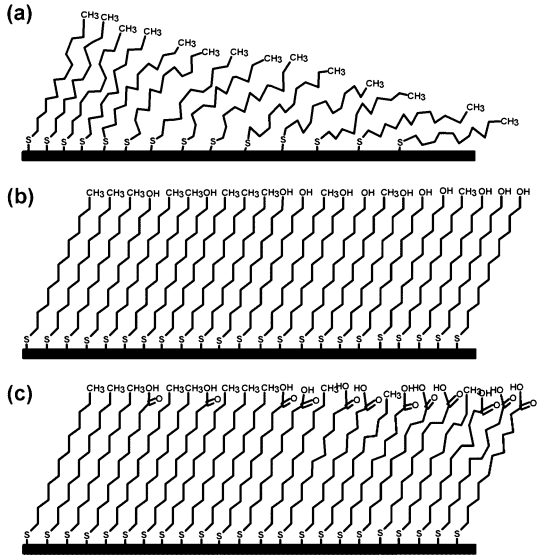

Figure 8. Schematic depiction of the structure of (a) a single-component dodecanethiol gradient and a two-component gradient with (b) 11-mercaptoundecanol or (c) 11-mercaptoundecanoic acid. The alkyl chains in the methyl-hydroxyl gradient (b) are well ordered, whereas in a methyl-carboxyl gradient (c) there is an increased disorder at the carboxyl end. The figure is meant to be illustrative and is not a quantitative description of conformational disorder.

This could be due to the contribution to this intensity from other species such as water molecules bound to the carboxyl groups. Also, the intensity around 1400 cm^{-1} is further complicated by the presence of several possible bands (e.g., deformation of COOH, scissoring modes of CH_2, stretching modes of COO^-). A quantitative differentiation of the ratio of carboxylic to carboxylate from these intensities was difficult, owing to the presence of multiple peaks in this region.

Conclusions

Surface-chemical gradients on centimeter length scales with different end-groups have been prepared by a simple two-step immersion method. The single-component gradient of dodecanethiol resulting after the first immersion step is composed of a disordered lying-down phase at the low-concentration end, gradually changing into a disordered standing-up phase at the higher-concentration end. Upon back-filling such a gradient with either 11-mercaptoundecanol or 11-mercaptoundecanoic acid, a complete monolayer, exhibiting almost linear variations in surface concentration of either hydroxyl or carboxyl functionality, is formed. The gradient composed of methyl- and hydroxyl-terminated thiols shows a well-ordered structure along the entire length of the sample, whereas the methyl-carboxyl gradient shows an increased conformational disorder at the carboxyl-rich end. The carboxyl groups in a methyl-carboxyl gradient prepared from ethanol are present as carboxylate ions, which could be converted to carboxylic acid by rinsing with acidified ethanol. The proposed structures of the single- and two-component gradients are shown as a schematic representation (Figure 8). Gradients of alkanethiols with other ionizable end-groups are currently being investigated.

LA053302T